

Kinematic Singularity Analysis of a 5DOF Serial Robot Using the Denavit–Hartenberg Method

Dao Van Duong

Ho Chi Minh City University of Industry and Trade, HCM city, Vietnam.

Email address: duongdv@huit.edu.vn

Abstract - This study presents a comprehensive analysis method for the kinematic singularities of a five degrees of freedom (5DOF) industrial space robot with a PRRPR structure, comprising two translational joints and three rotational joints. The robot is designed with a base translational axis, a rotational joint around the vertical axis, two hinged rotational joints, and a translational joint that changes the reach of the arm, thus forming an unconventional sequential structure suitable for industrial tasks with large workspaces. The geometric model is constructed using the Denavit–Hartenberg (DH) method, from which the homogeneous transformation matrices, forward kinematic equations, and the posture of the end effector are fully established. Based on the selection of a five-dimensional task space, including three position components and two independent orientation components, the Jacobian matrix is established and analyzed through rank attenuation conditions, determinants, and singularity values. The results show that the physically feasible singular configurations mainly depend on the angular position of the vertical rotational joint. Two main singularities appear when the entire arm assembly aligns with the base translation axis in opposite directions. In these configurations, the movement of the base translation joint becomes linearly dependent on the movement of the upper link chain, causing the robot to lose an independent velocity direction at the point of operation. Analysis also shows that the singularity neighborhood can cause a sharp increase in joint velocity, increased drive load, decreased trajectory tracking accuracy, reduced Cartesian stiffness, and numerical instability in the inverse kinematics problem. The singularity conditions were verified by numerical simulation and three-dimensional visualization. The research results provide a scientific basis for workspace partitioning, trajectory planning to avoid singularities, safe control design, and actuator protection in welding, grinding, inspection, additive manufacturing, and machine tool servicing applications.

Keywords—PRRPR robot, Denavit–Hartenberg, Forward kinematics, Jacobian, Kinematic singularity.

I. INTRODUCTION

Robots and industrial robotic arms are core components of automated production systems, enabling the performance of repetitive tasks requiring high precision or occurring in environments unfavorable to humans. Compared to robotic arms using only rotary joints, robots combining rotary and translational joints have the ability to significantly expand the workspace, create direct linear motion, and flexibly adjust the reach of the mechanism. Rotary joints ensure the ability to change the direction and posture of the working head, while translational joints are particularly suitable for tasks requiring long travel, approach along a defined direction, or serve multiple positions on the same production line. This combination is valuable in welding, mechanical processing,

inspection, pick-and-place, additive manufacturing, and machine tool servicing. Domestic studies on machining robots have shown an increasing demand for accuracy, error compensation capabilities, and control quality when robots are subjected to changing technological forces and dynamic parameters [1, 2]. At the same time, research on serial-parallel hybrid robotic arms shows that combining multiple kinematic chain types can simultaneously take advantage of workspace, stiffness and configuration flexibility [3]. However, hybrid structures also increase the complexity of the kinematic model, the linkage between joint movements and the risk of developing configurations that degrade controllability.

Mathematical modeling is the basis for describing the relationship between joint variables and the position of the manipulator point, and also serves simulation, trajectory planning, and control design. For serial robotic arms, the Denavit–Hartenberg method is often used to establish the coordinate system, build homogeneous transformation matrices, and solve the forward kinematics problem. However, the accuracy of the results depends significantly on how the coordinate system is attached, the positive direction convention, and the correct determination of geometric parameters. Recent studies have systematized first- and second-order differential kinematics, in which the Jacobian plays the role of mapping joint velocity to manipulator point velocity, while the derivatives of the Jacobian and Hessian are used in acceleration analysis [4, 5]. Comparison of analytical models, simulation software, and optimization methods also shows the need for cross-validation of models to limit setup errors and calculation errors [6]. On the basis of forward kinematics, singularities are determined when the Jacobian rank decays, losing the one-to-one mapping relationship between joint motion and head motion. For six-degree-of-freedom industrial robots and redundantly driven robots, studies have used determinants, rank analysis, matrix transformations, and singularity value decomposition to determine singularity conditions [7, 8]. This analysis has direct implications for establishing the safe working domain, selecting configurations, and preventing abnormal increases in joint velocity.

In robots with both rotary and translational joints, singularities not only appear when the rotating links are aligned but can also arise when the direction of motion of a translational joint becomes linearly dependent on the velocity generated by other joints. Therefore, identifying singularities by geometric observation is often insufficient, especially when the joint axes are arranged perpendicular or parallel in space. Studies of mechanisms containing rotary-translational pairs show that it is

necessary to consider instantaneous kinematics, workspace and singularity-free domain simultaneously instead of just evaluating geometric approachability [9]. For redundant robots, empty space projection can be used to maintain the main task and adjust the secondary configuration, but the orientation representation itself can also create algorithmic singularities or reduce the effectiveness of singularity avoidance [10]. Pseudo-inverse methods support the inverse kinematics solution for redundant robots, but solutions can become sensitive and difficult to satisfy simultaneously the joint limits, collision avoidance and continuity of motion [11]. 5- or 6-axis robots may also require workspace separation and task prioritization to overcome singularities without causing excessive joint velocity [12]. The main challenges therefore include distinguishing geometric singularities from representational singularities, handling non-square Jacobians, ensuring solution continuity, limiting joint velocity-acceleration, and maintaining workpiece accuracy when the robot operates near the loss region.

Recent works show that most singularity research focuses on pure rotary serial robots with six or seven degrees of freedom, parallel robots, continuous robots, and super-redundant systems. Meanwhile, the number of studies presenting analytical singularity conditions for spatial serial robots with interlocking rotary and translational joints is still relatively limited. This is an observation drawn from the scope of the surveyed literature, not an assertion that there is absolutely no research on this type of mechanism. Some domestic works have studied inverse dynamics and oscillation control for robotic arms with translational-rotational motion, but the focus is mainly on softness, oscillation, and dynamic load rather than a complete classification of singularity families [13]. Modern kinematic control methods for super-redundant robots often focus on solving the optimization problem under the joint velocity limit, thereby showing that singularity and near-singularity regions are still important constraints for the viability and stability of the solution [14]. For robots with length-changing or extendable links, the inverse kinematic model must also simultaneously handle geometric constraints, trajectories, and multiple feasible solutions [15]. Therefore, separate study of the PRRPR structure is necessary to determine the relationship between joint axis arrangement and Jacobian rank loss, distinguish mathematical singularities from feasible singularities in mechanical limits, and build a basis for trajectory planning and singularity avoidance control.

This study proposes the construction of a complete kinematic model for a five-degree-of-freedom PRRPR space robot, in which two translational and three rotational joints are arranged in an interlocking manner according to defined axis relationships. First, local coordinate systems are established using the Denavit–Hartenberg method to construct the transformation matrix between the links and the forward kinematic equations of the manipulator. Next, a five-dimensional task space suitable for the robot's actual positioning and orientation capabilities is determined, from which the task Jacobian is established. Singular conditions are derived by determinant analysis, matrix rank, and minimum singular value, and are compared with the physical limits of the

joints. Possible singular configurations will be represented by the coordinates of the workpiece, joint variables, and a three-dimensional spatial model. Finally, the influence of the near singularity region on joint velocity, accuracy, and trajectory tracking capability was evaluated using MATLAB simulations, providing a basis for proposing a safe working region and trajectory planning strategy to avoid singularities.

II. MATERIALS AND METHODS

2.1 Kinematics modelling

For a 5-DOF robotic arm model (PRRPR) as shown in Fig 1. It depicts a 5DOF spatial articulated robot consisting of five links connected by five joints in a PRRPR configuration, where joints 1 and 4 are translational joints, while joints 2, 3, and 5 are rotational joints. The first translational joint (q_1) moves the entire robot assembly along the base rail ($AB = L_0$). Link 2 is a vertical column with length (L_2), connected to the base by a rotational joint (q_2); link 3 has length (L_3) and rotates around a hinge joint (q_3); link 4 is a translational link with maximum geometric length ($CO_5 = L_4$), where the instantaneous length from (O_4) to (O_5) is equal to ($L_4 - q_4$); link 5 has length ($L_5 = O_5E$) and rotates around a hinge joint (q_5). The fixed coordinate system ($OXYZ$)₀ has its origin (O_0) at point (A), the axis (X_0) is horizontal along the rail, and the axis (Z_0) is vertical. System ($OXYZ$)₁ has its origin (O_1) coinciding with (O_0), where the axis (Z_1) coincides with (X_0). System ($OXYZ$)₂ has its origin (O_2) at the foot of the vertical link and the axis (Z_2) is parallel to (Z_0). System ($OXYZ$)₃ is located at (O_3), at the top end of link 2, with (Z_3) perpendicular to (Z_2). System ($OXYZ$)₄ is located at (O_4), with (Z_4) along the translational link and perpendicular to (Z_3). System ($OXYZ$)₅ is located at (O_5), where (Z_5) is perpendicular to (Z_4) and parallel to (Z_3), and (X_5) is along the last link.

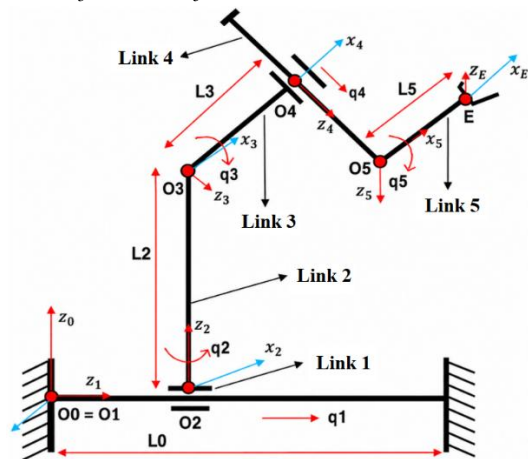


Figure 1. PRRPR model

Accordingly, the Denavit–Hartenberg specifications table is established as Tab 1.

Table 1. DH parameters

| Links | θ_i | d_i | a_i | α_i |
|-------|------------|-------------|-------|------------|
| 1 | 0 | q_1 | 0 | $\pi/2$ |
| 2 | q_2 | L_2 | 0 | $-\pi/2$ |
| 3 | q_3 | 0 | L_3 | $\pi/2$ |
| 4 | 0 | $L_4 - q_4$ | 0 | $-\pi/2$ |
| 5 | q_5 | 0 | L_5 | 0 |

The convention is as follows: $c_i = \cos q_i$, $s_i = \sin q_i$, $c_{35} = \cos(q_3 + q_5)$, $s_{35} = \sin(q_3 + q_5)$. The homogeneous transformation matrices from coordinate system i-1 to coordinate system i (i=1,..., 5) are shown as follows

$$\begin{aligned}
 \mathbf{H}_1 &= \begin{bmatrix} 1 & 0 & 0 & 0 \\ 0 & 1 & 0 & 0 \\ 0 & 0 & 1 & 0 \\ 0 & 0 & 0 & 1 \end{bmatrix}, & \mathbf{H}_2 &= \begin{bmatrix} 1 & 0 & -1 & 0 \\ 0 & c_2 & 0 & 0 \\ 0 & s_2 & 0 & q_1 \\ 0 & 0 & 0 & 1 \end{bmatrix} \\
 \mathbf{H}_3 &= \begin{bmatrix} 1 & s_3 & 0 & 0 \\ 0 & c_3 & 0 & 0 \\ 0 & 0 & 1 & L_2 \\ 0 & 0 & 0 & 1 \end{bmatrix}, & \mathbf{H}_4 &= \begin{bmatrix} 1 & 0 & L_3 & 0 \\ 0 & 0 & 0 & 0 \\ 0 & 1 & 0 & 0 \\ 0 & 0 & 0 & 1 \end{bmatrix} \\
 \mathbf{H}_5 &= \begin{bmatrix} 1 & s_5 & c_5 & 0 \\ 0 & c_5 & s_5 & 0 \\ 0 & 0 & 0 & L_4 - q_4 \\ 0 & 0 & 0 & 1 \end{bmatrix}
 \end{aligned} \tag{1}$$

The homogeneous transformation matrix between local coordinate systems and fixed coordinate systems is defined as follows

$$\begin{aligned}
 \mathbf{D}_1 = \mathbf{H}_1 &= \begin{bmatrix} 1 & 0 & 0 & 0 \\ 0 & 1 & 0 & 0 \\ 0 & 0 & 1 & 0 \\ 0 & 0 & 0 & 1 \end{bmatrix}, & \mathbf{D}_2 &= \begin{bmatrix} 1 & -s_2 & 0 & q_1 \\ 0 & c_2 & 0 & 0 \\ 0 & 0 & 1 & 0 \\ 0 & 0 & 0 & 1 \end{bmatrix} \\
 \mathbf{D}_3 &= \begin{bmatrix} c_2 c_3 & c_2 s_3 & -s_2 & q_1 \\ c_2 c_3 & s_2 s_3 & c_2 & 0 \\ s_3 & -c_3 & 0 & L_2 \\ 0 & 0 & 0 & 1 \end{bmatrix}, \\
 \mathbf{D}_4 &= \begin{bmatrix} c_2 s_3 & -s_2 & c_2 c_3 & q_1 + L_3 c_2 c_3 \\ c_2 s_3 & c_2 & s_2 c_3 & L_3 s_2 c_3 \\ c_3 & 0 & s_3 & L_2 + L_3 s_2 \\ 0 & 0 & 0 & 1 \end{bmatrix} \\
 \mathbf{D}_5 &= \begin{bmatrix} c_2 c_{35} & c_2 s_{35} & -s_2 & q_1 + R_4 c_2 c_3 \\ c_2 c_{35} & s_2 s_{35} & c_2 & R_4 s_2 c_3 \\ s_{35} & -c_{35} & 0 & L_2 + R_4 s_2 \\ 0 & 0 & 0 & 1 \end{bmatrix}
 \end{aligned} \tag{2}$$

Note that: $R_4 = L_3 + L_4 - q_4$. The kinematic equations are specifically defined as follows:

$$X_{0E} = q_1 + \cos q_2 [(L_3 + L_4 - q_4) \cos q_3 + L_5 \cos(q_3 + q_5)] \tag{3}$$

$$Y_{0E} = \sin q_2 [(L_3 + L_4 - q_4) \cos q_3 + L_5 \cos(q_3 + q_5)]$$

$$Z_{0E} = L_2 + (L_3 + L_4 - q_4) \sin q_3 + L_5 \sin(q_3 + q_5).$$

The direction of the end-effector link is determined as follows

$${}^0R_E = \begin{bmatrix} c_2 c_{35} & c_2 s_{35} & -s_2 \\ c_2 c_{35} & s_2 s_{35} & c_2 \\ s_{35} & -c_{35} & 0 \end{bmatrix} \tag{4}$$

2.3 Identifying Kinematic Singularities

Based on the kinematic model of the system with alternating rotary and translational joint types, the kinematic singularity must be determined from the Jacobian rank reduction, not just from the position of the structure as in the usual physical structure consideration. For a 5-DOF robot, the natural task space is chosen as $x_E = [X_{0E} \ Y_{0E} \ Z_{0E} \ \psi_E \ \theta_E]^T$, with $\psi_E = q_2$ and $\theta_E = q_3 + q_5$. The joint variable vector is $\mathbf{q} = [q_1 \ q_2 \ q_3 \ q_4 \ q_5]^T$. Accordingly, the Jacobian is defined as:

$$\dot{x}_E = \mathbf{J}_t(\mathbf{q}) \dot{\mathbf{q}} \tag{5}$$

So,

$$\mathbf{J}_t = \frac{\nabla (X_{0E}, Y_{0E}, Z_{0E}, \psi_E, \theta_E)}{\nabla (q_1, q_2, q_3, q_4, q_5)} \tag{6}$$

Let:

$$\eta = a \sin q_3 + L_5 \sin(q_3 + q_5), \quad \rho = a \cos q_3 + L_5 \cos(q_3 + q_5).$$

Then,

$$\mathbf{J}_t = \begin{bmatrix} -\rho \sin q_2 & -\eta \cos q_2 & -\cos q_2 \cos q_3 & -L_5 \cos q_2 \sin(q_3 + q_5) \\ \rho \cos q_2 & -\eta \sin q_2 & -\sin q_2 \cos q_3 & -L_5 \sin q_2 \sin(q_3 + q_5) \\ 0 & \rho & -\sin q_3 & L_5 \cos(q_3 + q_5) \\ 1 & 0 & 0 & 0 \\ 0 & 1 & 0 & 1 \end{bmatrix} \tag{7}$$

The Jacobian determinant is defined as follows

$$\det \mathbf{J}_t = (L_3 + L_4 - q_4) \sin q_2 \tag{8}$$

Therefore, a singularity occurs when $(L_3 + L_4 - q_4) \sin q_2 = 0$.

That is, one of two conditions: $\sin q_2 = 0$ or $L_3 + L_4 - q_4 = 0$.

It is easy to see that condition $L_3 + L_4 - q_4 = 0$ cannot occur because $L_3 + L_4 - q_4 > L_3 > 0$.

Consider the first singularity $S_1 : q_2 = 0$. At this time, the joint configuration is $\mathbf{q}_{S_1} = [q_1 \ 0 \ q_3 \ q_4 \ q_5]^T$. The coordinates of the operation point E are determined as follows:

$$\begin{aligned}
 X_{0E}^{(S_1)} &= q_1 + (L_3 + L_4 - q_4) \cos q_3 + L_5 \cos(q_3 + q_5) \\
 Y_{0E}^{(S_1)} &= 0
 \end{aligned} \tag{9}$$

$$Z_{0E}^{(S_1)} = L_2 + (L_3 + L_4 - q_4) \sin q_3 + L_5 \sin(q_3 + q_5)$$

The geometric parameters are specified as follows: $L_0 = 1(m); L_2 = 0.8(m); L_3 = 0.5(m); L_4 = 0.6(m); L_5 = 0.3(m)$, $0 < q_1 < L_0; 0 < q_4 < L_4$. Fig 2 illustrates the robot's position relative to this first singularity.

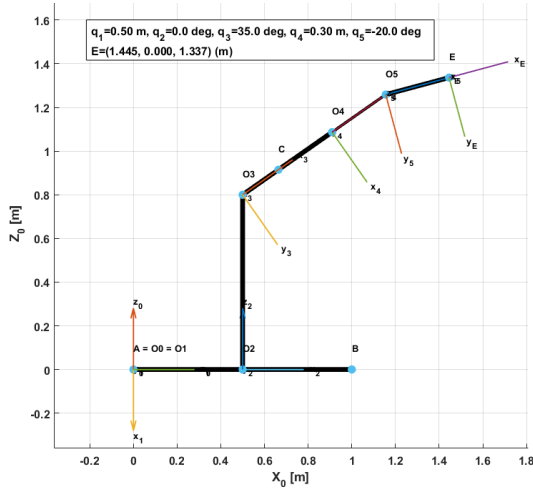


Figure 2. Robot configuration at the first singularity

In the first singular configuration S_1 , the vertical pivot joint has a value of $q_2 = 0$, so the upper arm assembly is oriented toward the positive side of the axis X_0 and the entire chain of links from O_3 to the operating point E lies in the plane $(OXZ)_0$. The coordinates of point E are then determined by $(Y_{0E} = 0)$ while X_{0E} is equal to the sum of the displacements of the base translational joint q_1 , the horizontal projection component of the equivalent link segment from O_3 to O_5 , and the projection component of the end link L_5 . The coordinates Z_{0E} depend on the fixed height L_2 , the lift angle q_3 , the resultant angle $(q_3 + q_5)$ and the effective length influenced by q_4 . The orientation of the axis X_5 , which is also the orientation of the end effector, is determined by the combined elevation angle $(q_3 + q_5)$ in the plane $(OXZ)_0$. Geometrically, this configuration makes the direction of movement of joint q_1 coincide with the radial direction of the robot arm. Therefore, part of the movement generated by the base translational joint becomes linearly dependent on the movement generated by joints q_3, q_4 and q_5 . Physically, the robot does not completely lose its mobility, but loses an independent velocity direction in the five-dimensional task space. Near this configuration, the inverse kinematic solver may require very high joint velocities to produce a small Cartesian velocity, causing servo saturation, increased current, vibration, and trajectory tracking errors. In welding, grinding, or additive printing applications, the degradation of controllability can result in uneven workpiece speed, oscillating approach angle, and reduced process quality. Therefore, S_1 should be considered an unsafe configuration boundary for tasks requiring high positional and orientational accuracy simultaneously.

Consider the second singularity $S_2 : q_2 = \pi$. At this point, the joint configuration is $\mathbf{q}_{S_2} = [q_1 \ \pi \ q_3 \ q_4 \ q_5]^T$. The coordinates of the operation point E are determined as follows:

$$X_{0E}^{(S_2)} = q_1 - [(L_3 + L_4 - q_4) \cos q_3 + L_5 \cos(q_3 + q_5)] \quad (10)$$

$Y_{0E}^{(S_2)} = 0$
 $Z_{0E}^{(S_2)} = L_2 + (L_3 + L_4 - q_4) \sin q_3 + L_5 \sin(q_3 + q_5)$
 The configuration of robot at the second singular position is shown in Fig 3.

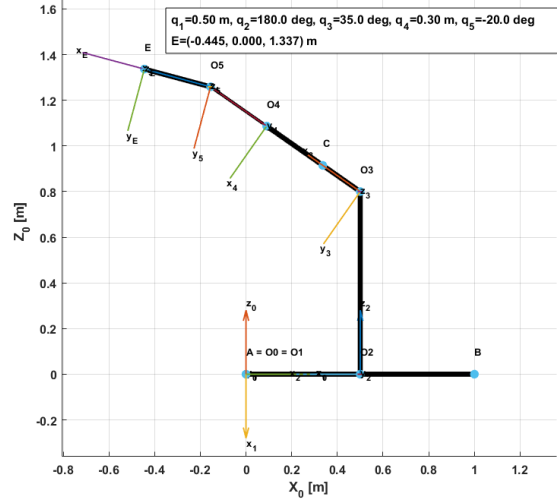


Figure 3. Robot configuration at the second singularity.

In the second singular configuration S_2 , the vertical pivot joint reaches a value $q_2 = \pi$, causing the arm assembly to rotate in the opposite direction and towards the negative side of the axis X_0 . Similar to case S_1 , the operating point (E) remains in the plane $(OXZ)_0$, so $Y_{0E} = 0$. However, the coordinate X_{0E} is determined by the displacement q_1 minus the horizontal projection component of the upper link chain, reflecting the robot arm opening towards the opposite side of the positive direction of the base rail. The coordinate Z_{0E} does not change in form compared to case $q_2 = 0$, because the height of the working head is still determined by L_2 , angle q_3 , total angle $(q_3 + q_5)$, effective length of the translational link and length of the end link. The direction of the manipulator remains in the plane $(OXZ)_0$, but its horizontal component is reversed compared to configuration S_1 . The important geometric meaning is that the radial direction of the arm chain is now opposite to the positive movement of the joint q_1 , but the two directions still lie on the same line of action. Therefore, the corresponding columns in the Jacobian continue to become linearly dependent, reducing the matrix rank. Physically, this phenomenon can cause large internal movement but very small displacement of point (E), especially when q_1 and the uppermost joints change in opposite directions. The drive system then consumes unnecessary energy, increasing friction, and putting load on the screw, guide rails, and gearbox. In practice, configuration S_2 may occur when the robot serves work areas behind the rail or when the trajectory requires the arm to rotate more than half a turn. Without a suitable kinematic branch selection strategy, the robot may change configuration abruptly, causing jerks, increased joint acceleration, and reduced manipulation accuracy. Therefore, it is necessary to

limit the technological trajectory from directly passing through the vicinity $q_2 = \pi$.

Consider the series of singularities $S_k : q_2 = k\pi$. So, $\cos(k\pi) = (-1)^k$, $\sin(k\pi) = 0$. Therefore:

$$\begin{aligned} X_{0E}^{(k)} &= q_1 + (-1)^k \begin{pmatrix} L_3 + L_4 - q_4 \\ L_5 \end{pmatrix} \cos(q_3 + q_5) \\ Y_{0E}^{(k)} &= 0 \end{aligned} \quad (11)$$

$$Z_{0E}^{(k)} = L_2 + (L_3 + L_4 - q_4) \sin q_3 + L_5 \sin(q_3 + q_5)$$

The two configurations S_1 and S_2 are essentially representative cases of the generalized singularity family $q_2 = k\pi$, where k is an integer. When k is even, the robot arm points toward the positive side of the axis X_0 ; when k is odd, the arm points toward the negative side of this axis. In all cases, the coordinate Y_{0E} is zero, indicating that the manipulator lies on the plane of symmetry $(OXZ)_0$. The coordinate X_{0E} changes sign according to the evenness-oddness of k , while the coordinate Z_{0E} remains unchanged depending on the variables q_3, q_4 and q_5 . The direction of the manipulator link is determined by the total lift angle and rotates periodically according to the variation of q_2 , but at every value of $k\pi$, the horizontal direction of the arm is always aligned with the translational rail. Geometrically, these are not a finite number of distinct points but rather a continuous family of singular configurations, because at each value $q_2 = k\pi$, the remaining variables can still take many values within the mechanical limits. Therefore, in joint space, singularities form hypersurfaces that divide the working domain into different configuration regions. Physically, as the robot approaches any element of this singularity family, the smallest Jacobian singularity value decreases, the condition coefficient increases, and the ability to switch between Cartesian velocity and joint velocity decreases. Encoder errors, play, friction, and elastic deformation can be amplified, making the workpiece more sensitive to noise and external forces. In particular, in force control or contact machining, Cartesian stiffness can decrease sharply in some directions, leading to force oscillations and positional errors. This singularity family also makes the inverse kinematics problem prone to losing its uniqueness or shifting the solution branch. Therefore, the analysis needs to be performed not only at the exact location $q_2 = k\pi$, but also in a neighborhood defined by the minimum singularity threshold, condition coefficient, or manipulability index.

Analysis of the two representative configurations and the generalized singularity family reveals that the core cause of the singularity in the PRRPR robot under consideration is the alignment between the direction of movement of the base translational joint and the radial direction of the upper arm chain. In the physical working domain, the effective length related to q_4 is always positive, so the singularity is mainly governed by the rotation angle q_2 . This facilitates monitoring, but should not lead to a simple solution by simply eliminating the two values 0 and π . In practice, the region near the

singularity is the area that poses the most risk, because the robot can still move but its velocity, acceleration, and joint torque increase sharply, while accuracy, stiffness, and noise immunity decrease. For trajectory programming, a safety margin should be set for q_2 , and a penalty function based on the smallest singularity value, condition coefficient, or maneuverability index should be added to the optimization problem. The trajectory should be redistributed between q_1 , q_3 , and q_4 to avoid bringing the arm plane into alignment with the base rail. In inverse kinematics, direct Jacobian inversion should not be used; instead, damped pseudo-inversion, constrained square optimization, or task-priority control should be applied. The controller should integrate velocity, acceleration, jerk, torque, and current limits, and automatically decelerate when the singularity approaches a dangerous threshold. For contact tasks such as grinding, polishing, or inspection, additional monitoring of force, stiffness, and workpiece oscillation is required. In terms of application, the workpiece, fixture, and approach direction should be arranged so that the robot operates primarily in the high-maneuverability region, avoiding the need for the arm to change direction directly via $q_2 = 0$ or $q_2 = \pi$. An approach combining work area design, trajectory planning, and adaptive control will improve safety, accuracy, and drive life.

III. CONCLUSION

This study has developed a complete mathematical model for a five-degree-of-freedom PRRPR articulated robot, in which translational and rotational joints are arranged in an interlocking manner according to defined geometric relationships. Based on the Denavit–Hartenberg method, local coordinate systems, homogeneous transformation matrices, and forward kinematic equations of the workpiece have been established, thereby clearly describing the relationship between joint variables, position, and orientation of the workpiece. From the kinematic model, a five-dimensional task Jacobian was constructed to evaluate the velocity transfer capability between joint space and workpiece space. Analysis results show that the singularity of the mechanism mainly appears when the vertical rotational joint brings the entire arm assembly in alignment with the base translational axis in two opposite directions. In these configurations, the movement of the first translational joint becomes linearly dependent on the movement created by the upper link chain, causing the robot to lose an independent velocity direction. The analysis also indicates that the travel limits of the translational joint do not directly create geometric singularities in the physical working domain, but can impair the ability to adjust the configuration and increase the risk of operating near the singularity. These results have significant implications for workspace partitioning, posture selection, and safe trajectory construction. In subsequent studies, the inverse kinematics problem should utilize damped pseudo-inverse or constrained optimization to limit large joint velocities near the singularity. The dynamic model needs to incorporate the influence of inertia, friction, flexibility, and workpiece load to accurately assess the forces and torques transmitted. Regarding control, it is necessary to integrate singularity index monitoring,

velocity-acceleration-jerk limiting, and adaptive deceleration mechanisms. In practical applications, the workpiece, approach direction, and operating area should be positioned so that the robot avoids linear configurations, thereby improving the accuracy, stability, and durability of the drive system.

REFERENCES

- [1] Khoi, P. B. (2024). Integration of genetic algorithm and Hedge Algebras in controlling mechanical machining robots. *Vietnam Journal of Mechanics*, 46(2), 163–180. <https://doi.org/10.15625/0866-7136/21000>
- [2] Khoi, P. B., Hai, H. T., & Thuy, T. M. (2023). An error compensation controller for milling robots. *Vietnam Journal of Mechanics*, 45(2), 105–116. <https://doi.org/10.15625/0866-7136/16979>
- [3] Yun, X., Zhao, T., Zhu, B., Pang, D., Yang, C., & Qi, J. (2025). Research on redundant control of serial-parallel hybrid multi-robot ship-dock system. *Ocean Engineering*, 340, 122191. <https://doi.org/10.1016/j.oceaneng.2025.122191>
- [4] Ziao, M., Zhang, Y., Fu, H., & Wang, Z. (2018). Nonlinear unbiased minimum-variance filter for Mars entry autonomous navigation under large uncertainties and unknown measurement bias. *ISA Transactions*, 76, 97–109. <https://doi.org/10.1016/j.isatra.2018.02.010>
- [5] Zhu, W., & Li, B. (2024). EM-aided fast posterior covariance computation in Bayesian FFT method. *Mechanical Systems and Signal Processing*, 211, 111211. <https://doi.org/10.1016/j.ymssp.2024.111211>
- [6] Elhadidy, M. S., Abdalla, W. S., Abdelrahman, A. A., Elnaggar, S., & Elhosseini, M. (2024). Assessing the accuracy and efficiency of kinematic analysis tools for six-DOF industrial manipulators: The KUKA robot case study. *AIMS Mathematics*, 9(6), 13944–13979. <https://doi.org/10.3934/math.2024678>
- [7] Diego, P., Macho, E., Campa, F. J., Herrero, S., Diez, M., Corral, J., & Pinto, C. (2026). Singularity conditions from a kinetostatic analysis of a new parallel robot for human balance and gait rehabilitation. *Mechanism and Machine Theory*, 219, 106328. <https://doi.org/10.1016/j.mechmachtheory.2025.106328>
- [8] Wang, M., Xiao, J., Zhao, W., Hou, R., & Liu, H. (2026). Online trajectory scaling for singularity traversal in 5-DOF hybrid robots. *Mechanism and Machine Theory*, 225, 106456. <https://doi.org/10.1016/j.mechmachtheory.2025.106456>
- [9] Milenkovic, P., Wang, Z., & Rodriguez, J. I. (2026). Encircling singularities of a serial robot to find alternative inverse-kinematic solutions. *Mechanism and Machine Theory*, 219, 106314. <https://doi.org/10.1016/j.mechmachtheory.2025.106314>
- [10] Schappler, M., & Ortmaier, T. (2021). Singularity avoidance of task-redundant robots in pointing tasks: On nullspace projection and Cardan angles as orientation coordinates. In *Proceedings of the 18th International Conference on Informatics in Control, Automation and Robotics* (pp. 338–349). SCITEPRESS. <https://doi.org/10.5220/0010621103380349>
- [11] Hong, T., Li, W., & Huang, K. (2024). A reinforcement learning enhanced pseudo-inverse approach to self-collision avoidance of redundant robots. *Frontiers in Neurobotics*, 18, 1375309. <https://doi.org/10.3389/fnbot.2024.1375309>
- [12] Tajima, S., & Sencer, B. (2020). Real-time trajectory generation for 5-axis machine tools with singularity avoidance. *CIRP Annals - Manufacturing Technology*, 69(1), 349–352. <https://doi.org/10.1016/j.cirp.2020.04.113>
- [13] Khang, N. V., & Dat, D. C. (2022). Vibration control and calculating inverse dynamics of the rigid-flexible two-link manipulator T-R. *Vietnam Journal of Mechanics*, 44(2), 169–189. <https://doi.org/10.15625/0866-7136/16876>
- [14] Tang, Z., & Zhang, Y. (2022). Refined self-motion scheme with zero initial velocities and time-varying physical limits via Zhang neurodynamics equivalency. *Frontiers in Neurobotics*, 16, 945346. <https://doi.org/10.3389/fnbot.2022.945346>
- [15] Fritsch, S., & Oberschmidt, D. (2025). A projection-based inverse kinematic model for extensible continuum robots and hyper-redundant robots with an elbow joint. *Frontiers in Robotics and AI*, 12, 1627688. <https://doi.org/10.3389/frobt.2025.1627688>